

Special  
Collection

# TEMPO-Modified Polymethacrylates as Mediators in Electrosynthesis – Redox Behavior and Electrocatalytic Activity toward Alcohol Substrates

Nayereh Mohebbati,<sup>[a, b]</sup> Adrian Prudlik,<sup>[a, b]</sup> Anton Scherkus,<sup>[b]</sup> Aija Gudkova,<sup>[b]</sup> and Robert Francke\*<sup>[a, b]</sup>Dedicated to the memory of *Jean-Michel Savéant*.

Homogeneous catalysts (“mediators”) are useful for tuning selectivity in organic electrosynthesis. However, they can have a negative impact on the overall mass and energy balance if used only once or recycled inefficiently. In a previous work, we introduced the polymediator concept, in which soluble redox-active polymers catalyze the electrochemical reaction, allowing for recovery by dialysis or pressure-driven membrane filtration. Using anodic alcohol oxidation as a test case, it was shown that TEMPO-modified polymethacrylates (TPMA) can serve as efficient and reusable mediators. In the present study, the properties of a TPMA sample with well-defined molecular weight

distribution were studied using cyclic voltammetry and compared to low-molecular TEMPO species. The non-catalytic profiles of TPMA are shaped by diffusive and adsorptive processes, whereby the latter only become pronounced at low mediator concentrations and high scan rates. Electrocatalytic studies suggest that under the applied conditions, TPMA-catalyzed alcohol oxidation is a predominantly homogeneous process. The homogeneous kinetics are determined rather by the mediator potential than by steric influences of the polymer backbone.

In organic electrochemistry, indirect electrolysis using homogeneous catalysts (“mediators”) is a useful tool for shaping the course of the reaction and for reducing the energy consumption.<sup>[1]</sup> Consequently, mediators are widely used and find application both in *in-cell* processes (homogeneous electrocatalysis) and in *ex-cell* protocols (transformations with electro-generated reagents).<sup>[2]</sup> Another key advantage is that a variety of synthetic challenges can be addressed with a broad range of well-established mediators including organometallic compounds,<sup>[3]</sup> halide salts,<sup>[4]</sup> triarylaminines,<sup>[5]</sup> iodoarenes,<sup>[6]</sup> and *N*-oxyl radicals.<sup>[7]</sup> However, these positive features may be offset by additional costs, a more complex separation procedure, and increased waste generation, which is why concepts to improve separability and recyclability deserve more attention.<sup>[8]</sup>


The main cause of separation problems in indirect electrosynthesis is the similarity between mediator and product in


terms of polarity and molecular size. For example, column chromatography is necessary in protocols involving organo-mediators such as iodoarenes or 2,2,6,6-tetramethylpiperidinyl-1-oxyl (TEMPO). While this is not a particular problem on a laboratory scale, more straightforward methods such as extraction and filtration are required when scaling up. In this context, tuning of the mediator polarity by attaching charged groups (“ionic tags”) has turned out as a promising approach, facilitating recovery by extraction while eliminating the need for supporting electrolyte additives.<sup>[9]</sup> In further studies, mediator immobilization on suspended particles was attempted. Using poly(styrene)-supported phenyl iodide<sup>[10]</sup> and TEMPO attached to silica gel,<sup>[11]</sup> a straightforward recovery via simple filtration was achieved. However, the use of halide salts as co-mediators was necessary for activation of the immobilized mediator units, which is symptomatic for poor kinetics of the electron exchange between electrode and immobilized phenyl iodide units.


Compared to the dispersed-phase strategy, the attachment of a mediator to soluble polymer backbones (polymediators) leading to homogeneous electrolyte systems represents a promising approach. Such systems do not require a co-mediator and allow for recovery via size exclusion membrane processes (ultra-/ nanofiltration and dialysis).<sup>[12]</sup> Using the example of TEMPO-catalyzed alcohol oxidation as a test case, we have demonstrated for the first time that indirect electrosynthesis can be efficiently coupled to dialysis and ultrafiltration using polyelectrolyte HP-1 and polymediator HP-2 (see Figure 1). The polymer solutions are sufficiently conductive and exhibit a high electrocatalytic activity toward oxidation of various alcohols. Electrolysis on the preparative scale showed that various

[a] N. Mohebbati, A. Prudlik, Dr. R. Francke  
Leibniz Institute for Catalysis  
Albert-Einstein-Str. 29a, 18059 Rostock, Germany  
E-mail: robert.francke@catalysis.de

[b] N. Mohebbati, A. Prudlik, A. Scherkus, A. Gudkova, Dr. R. Francke  
Institute of Chemistry  
Rostock University  
Albert-Einstein-Str. 3a, 18059 Rostock, Germany

 Supporting information for this article is available on the WWW under <https://doi.org/10.1002/celec.202100768>

 An invited contribution to a joint Special Collection in memory of Prof. Jean-Michel Savéant.

 © 2021 The Authors. ChemElectroChem published by Wiley-VCH GmbH. This is an open access article under the terms of the Creative Commons Attribution Non-Commercial NoDerivs License, which permits use and distribution in any medium, provided the original work is properly cited, the use is non-commercial and no modifications or adaptations are made.

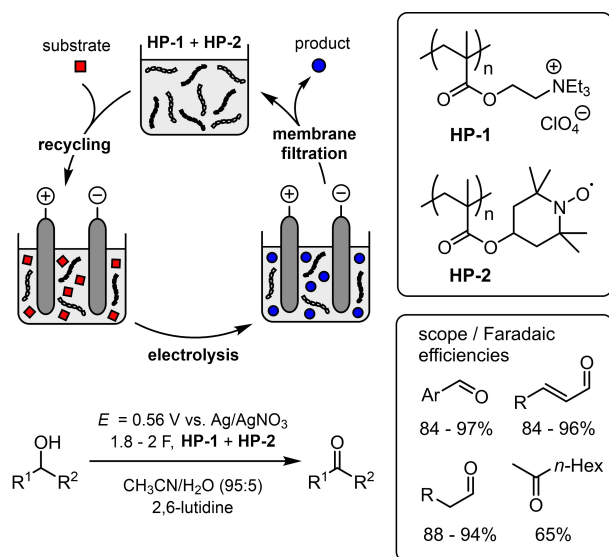


**Figure 1.** Summary of our previous study on the use of soluble polymediators and polyelectrolytes using the TEMPO-catalyzed oxidation of alcohols as a test case (Faradaic efficiencies determined after passing 1.8–2.0 charge equivalents).<sup>[12]</sup>

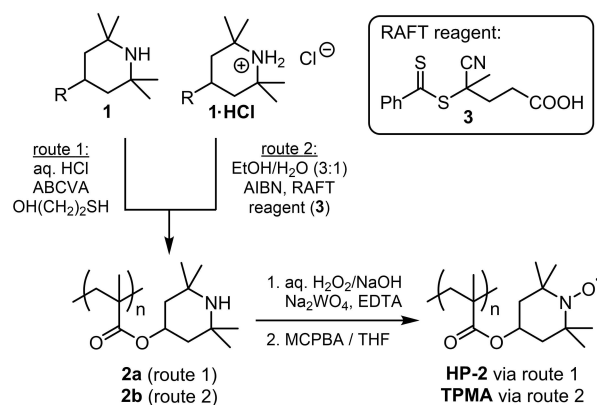
benzylic, allylic and aliphatic alcohols can be selectively converted to the corresponding carbonyl compounds, and that the electrolyte solution can be reused multiple times.

Initial cyclic voltammetry (CV) studies on a glassy carbon electrode showed that compared to “regular” TEMPO, the peak currents obtained for HP-2 under non-catalytic conditions are smaller, whereas the catalytic currents are significantly higher. Furthermore, the voltammetric response of the polymer exhibited some distinctive features, such as a peak-to-peak separation ( $\Delta E_p$ ) of 35 mV (at a scan rate of  $v = 50 \text{ mVs}^{-1}$ ), which is atypical both for adsorptive and diffusive behavior.<sup>[13]</sup> We believe that a better understanding of the voltammetry of polymediators is of high importance for future developments in the area of polymediated electrosynthesis. We have therefore carried out a detailed electroanalytical study on redox behavior and electrocatalytic properties of TEMPO-modified polymethacrylates, the results of which are presented herein.

## 1. Results and Discussion

### 1.1. Polymer Synthesis

In our previous work<sup>[12]</sup> we employed a free radical polymerization of commercially available 2,2,6,6-tetramethylpiperidin-4-yl-methacrylate (**1**) for the synthesis of precursor polymer **2a** (see Scheme 1, route 1).<sup>[14]</sup> 2-Mercaptoethanol was used as a modifier to lower the molar mass, to reduce the dispersity, and ultimately to guarantee sufficient solubility for electrochemical studies. A subsequent two-step oxidation with  $\text{H}_2\text{O}_2/\text{Na}_2\text{WO}_4$  (step 1) and MCPBA (step 2) yielded the desired TEMPO-modified polymer HP-2 with a mass average molecular weight ( $M_w$ ) of 2.74 kDa.<sup>[15]</sup> A simple experimental procedure and good



**Scheme 1.** Preparation of HP-1 and TPMA from monomer **1** (R = methacryloxy).

scalability are among the advantages of the method. However, the method features only a limited control over the length of the polymer chain, which is reflected by a relatively high dispersity ( $\mathcal{D} = 1.89$ ).

For the present study, we intended to reduce the dispersity to exclude possible influences of large molar mass differences. We achieved this goal by RAFT polymerization<sup>[16]</sup> of hydrochloride **1-HCl** using dithioester **3** as a chain transfer reagent (route 2). This approach, followed by oxidation of intermediate **2b** using the abovementioned two-step protocol, rendered the TEMPO-modified polymethacrylate (TPMA) in 87% yield with a higher molecular weight ( $M_w = 4.67 \text{ kDa}$ ) compared to HP-2 and to our delight, a much smaller dispersity ( $\mathcal{D} = 1.29$ ).<sup>[17]</sup> UV vis spectroscopic analysis indicates that intermediate **2b** contains intact thiobenzoylthio end groups, which are removed during conversion to TPMA. Cleavage under these reaction conditions is also in agreement with literature reports on the stability of thiobenzoylthio moieties.<sup>[18]</sup> Further details regarding synthesis and characterization are summarized in the supporting information (SI).

### 1.2. Redox Behavior Under Non-Catalytic Conditions

For the electrochemical characterization of TPMA, cyclic voltammetry (CV) was carried out in a 0.1 M solution of  $\text{NBu}_4\text{ClO}_4$  in  $\text{CH}_3\text{CN}/\text{H}_2\text{O}$  (8:1 vol/vol) using a glassy carbon working electrode and a  $\text{Ag}/0.01 \text{ M AgNO}_3$  reference electrode ( $E_0 = -87 \text{ mV}$  vs.  $\text{Fc}/\text{Fc}^+$  couple).<sup>[19]</sup> The polymer content was adjusted to a concentration of TEMPO units ( $c_{\text{TM}}$ ) of 5 mM.<sup>[20]</sup> To contrast the voltammetric behavior of TPMA against other *N*-oxyl radicals, we chose TEMPO as well as 4-acetoxy-TEMPO (ACT, Figure 2, top) for our studies. The CVs recorded at  $v = 100 \text{ mVs}^{-1}$  are shown in Figure 2 (bottom, for extracted parameters see Table 1). For each species, the scan reveals a single reversible redox couple ( $\text{R}_2\text{N}-\text{O}^*/\text{R}_2\text{N}=\text{O}^+$ ) with a typical diffusive profile. With respect to TPMA, this is well worth mentioning, as it suggests that there is no significant electronic coupling between the TEMPO motifs across the polymer chain,

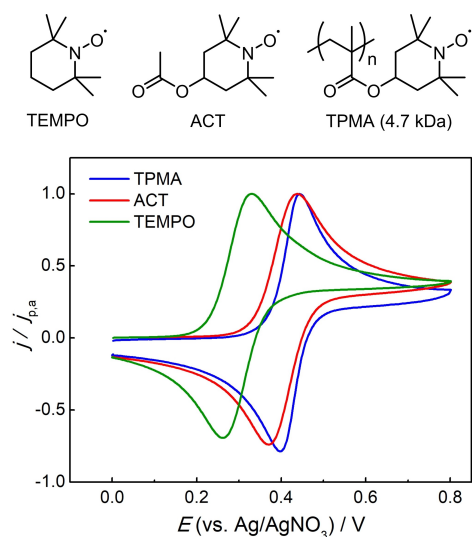


**Figure 2.** Top: Structures of the investigated mediators. Bottom: Background-corrected cyclic voltammetry (CV) of TEMPO, 4-acetoxy-TEMPO (ACT) and TEMPO-modified polymethacrylate (TPMA) normalized vs. the anodic peak current density  $j_{p,a}$ . Conditions: 0.1 M  $\text{NBu}_4\text{ClO}_4$  in acetonitrile/water (8:1),  $c_{\text{TU}} = 5 \text{ mM}$ ,  $v = 100 \text{ mV s}^{-1}$ .

**Table 1.** Summary of equilibrium redox potentials  $E_0$ , peak-to-peak separations  $\Delta E_p$ , anodic peak current densities  $j_{p,a}$ , and peak current ratios  $|j_{p,c}/j_{p,a}|$  obtained from the CVs shown in Figure 2 (bottom).

Compound	$E_0$ [V]	$\Delta E_p$ [mV]	$j_{p,a}$ [ $\text{mA cm}^{-2}$ ]	$ j_{p,c}/j_{p,a} $
TEMPO	0.30	69	1.94	1.0
ACT	0.40	67	1.73	1.0
TPMA	0.42	46	0.74	1.0

and that the redox characteristics at  $100 \text{ mV s}^{-1}$  are essentially the same as those displayed by the monomer.<sup>[21]</sup>

For TPMA (blue line), the redox couple is centered around  $E_0 = 0.42 \text{ V}$  with an anodic shift of 120 mV compared to free TEMPO (green line). The shift can be assigned to the presence of the acyloxy linker,<sup>[22]</sup> which is confirmed by comparison to the CV of structurally similar ACT (red line,  $E_0 = 0.40 \text{ V}$ ). There are also significant differences between the peak intensities: While ACT and TEMPO show comparable anodic peak current densities ( $j_{p,a}$ ), TPMA achieves only about 40% of these values. The latter indicates that the availability of TEMPO units at the electrode surface is lower, which may be attributed to slower mass transfer (*vide infra*). Full chemical reversibility on the voltammetry timescale is confirmed for TPMA, ACT and TEMPO by calculation of the ratio between the cathodic and the anodic peak current density  $|j_{p,c}/j_{p,a}|$  according to the method reported by Nicholson and Shain (for details see the SI).<sup>[23]</sup>

For TPMA, the presence of only one redox couple and the magnitude of the  $j_p$  values suggest that each polymer chain can be oxidized multiple times at the same potential, which is confirmed by a controlled potential coulometry experiment carried out at  $E = 0.6 \text{ V}$  in a divided cell (for details see the SI). The results show that at least 89% of the available TEMPO units

are oxidized before the current drops from the initial value of 1.6 mA to the baseline.<sup>[24]</sup>

Further differences between TPMA and ACT become apparent upon variation of  $v$  (Figure 3A and Figure 3B). While ACT exhibits a good linear correlation between  $j_{p,a}$  and  $v^{0.5}$  in the entire range, indicating a diffusive process,<sup>[25]</sup> for TPMA this is only the case between 5 and approx.  $250 \text{ mV s}^{-1}$  (Figure 3E). A possible explanation for the deviation of TPMA above  $250 \text{ mV s}^{-1}$  is a superposition of adsorptive and diffusive processes, i.e., charge transfer to both dissolved and adsorbed polymer chains. Thus, the square root dependency of  $j_p$  at low scan rates would indicate that at long time scales, the majority of the charge is transferred via diffusive processes. As the scan rate increases, the adsorptive fraction of  $j_p$  that increases linearly with  $v^{1/3}$  would become more pronounced. At this point, the  $v$  range dominated by the diffusive process is evaluated first to allow a comparison between the transport properties of the different *N*-oxyl species, while the unusual behavior of TPMA at high  $v$  will be discussed in detail below. The diffusion coefficients  $D$  were calculated from the slope of  $j_p$  versus  $v^{0.5}$  from Eq. 1,<sup>[25]</sup>

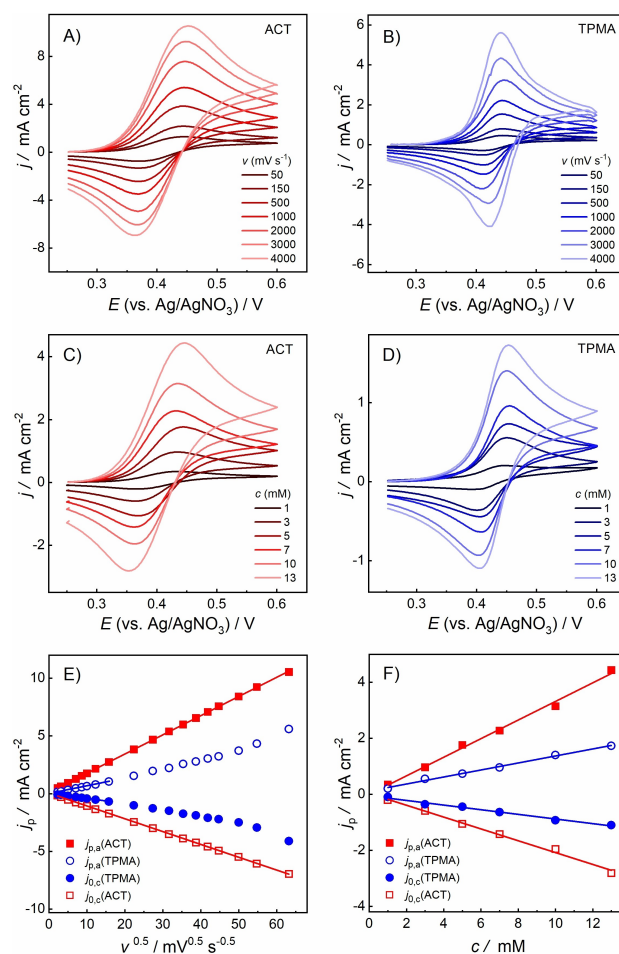


**Figure 3.** Top: Background-corrected voltammetry of ACT (A) and TPMA (B) at  $c_{\text{TU}} = 5 \text{ mM}$  and varying  $v$ . Middle: Background-corrected CVs of ACT (C) and TPMA (D) at  $100 \text{ mV s}^{-1}$  and varying  $c$ . Bottom: Comparison between the peak current densities ( $j_p$ ) of ACT and TPMA at varying  $v$  (E) and  $c_{\text{TU}}$  (F). Electrolyte: 0.1 M  $\text{NBu}_4\text{ClO}_4$  in acetonitrile/water (8:1).

$$j_p = 0.4463zF c_{TU} \sqrt{\frac{zFvD}{RT}} \quad (1)$$

where  $z$  is the number of transferred electrons ( $z=1$ ),  $F$  the Faraday constant,  $R$  the gas constant, and  $T$  the temperature (the other parameters are defined above). The results are summarized in Table 2 and more details are provided in the SI.

For TPMA, only the range between 5 and 250  $\text{mVs}^{-1}$  was analyzed, whereas the full range was used for ACT and TEMPO. With  $2.35 \cdot 10^{-6} \text{ cm}^2 \text{ s}^{-1}$ ,  $D_{\text{TPMA}}$  is one order of magnitude lower than  $D_{\text{TEMPO}}$  and approximately seven times smaller than  $D_{\text{ACT}}$ . The decrease in  $D$  follows the pattern predicted by the Stokes-Einstein equation in the sense that diffusion is curbed by increasing molecular size. The same effect is observed upon increasing  $c_{\text{TU}}$  (Figure 3C and Figure 3D), which also leads to a slower increase of  $j_p$  for TPMA as compared to ACT (Figure 3F).

To verify the assumption that adsorption of TPMA causes a deviation of  $j_p$  from the square root dependency, another experiment was performed in which CVs were first recorded at

Compound	slope [ $\text{mA s}^{0.5} \text{ cm}^{-2} \text{ mV}^{-0.5}$ ]	$D$ [ $\text{cm}^2 \text{ s}^{-1}$ ]
TEMPO	0.202	$2.26 \cdot 10^{-5}$
ACT	0.166	$1.53 \cdot 10^{-5}$
TPMA	0.065	$2.35 \cdot 10^{-6}$

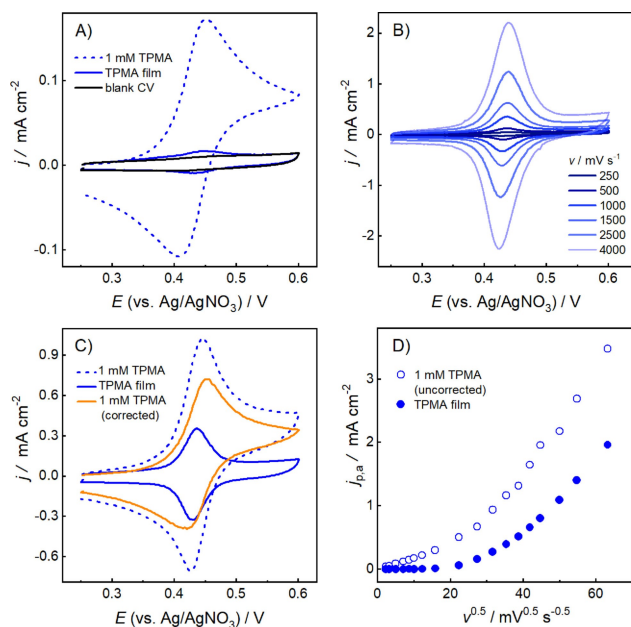


**Figure 4.** A) CV of 1 mM TPMA (dashed blue line) recorded at  $100 \text{ mVs}^{-1}$ , repeated scan after replacing the solution with blank electrolyte (solid blue line), and repeated scan after polishing the electrode (solid black line). B) CV of the TPMA film at various scan rates. C) CV of 1 mM TPMA recorded at  $1 \text{ Vs}^{-1}$  (dashed blue line), repeated scan in blank electrolyte (solid blue line), and CV of 1 mM TPMA after subtraction of adsorption contributions (solid orange line). D) Plot of  $j_p$  vs.  $v^{0.5}$  for 1 mM TPMA (hollow circles) and the TPMA film (filled circles). Electrolyte: 0.1 M  $\text{NBu}_4\text{ClO}_4$  in acetonitrile/water (8:1).

$c_{\text{TU}} = 1 \text{ mM}$  (see Figure 4A, dashed blue line), followed by careful rinsing of the glassy carbon electrode with acetonitrile, transfer to a blank electrolyte solution, and repeated cycling (Figure 4A, solid blue line). At  $100 \text{ mVs}^{-1}$ , the appearance of a redox couple with weak intensity and without peak-to-peak separation confirms irreversible adsorption of TPMA on the electrode surface. Increasing  $v$  leads to well-defined and nearly symmetric features centered around  $0.43 \text{ V}$  with very small splitting between the oxidative and the reductive peak ( $\Delta E_p \leq 10 \text{ mV}$ ), which is characteristic for identical and independent redox-active species attached to the electrode surface (Figure 4B).<sup>[25]</sup> At constant scan rate, the profiles do not significantly change over ten cycles (see Figure S7), indicating a good stability of the TPMA film on the voltammetry time scale. A control experiment in which the electrode was immersed into the TPMA-containing solution without applying a potential, followed by transfer to a blank electrolyte and cycling, gave similar results. This indicates that the adsorption process is not electrochemically induced but more likely due to a mixture of physisorption and low solubility of the polymer. Similar adsorption behavior was previously observed for other soluble redox-active polymers tested for energy storage applications.<sup>[26]</sup>

A comparison between the CVs of 1 mM TPMA and of the TPMA film at  $1 \text{ Vs}^{-1}$  confirms that at higher scan rates, the contribution of the TPMA film to the overall current response becomes more pronounced (Figure 4C), thus underlining the abovementioned responsibility of the adsorptive process for the deviations from the square root dependency. As expected, the deviation also increases with decreasing  $c_{\text{TU}}$  (compare  $c_{\text{TU}} = 1 \text{ mM}$  in Figure 4D with  $c_{\text{TU}} = 5 \text{ mM}$  in Figure 3E).

The key parameters extracted from the film CV recorded at  $1 \text{ Vs}^{-1}$  are summarized in Table 3. Both analysis of the anodic and cathodic peak charges ( $q_a$  and  $q_c$ ) and calculation of the peak current ratio indicates a high chemical reversibility of the adsorbed redox couple ( $q_c/q_a = 1.03$ ,  $j_{p,c}/j_{p,a} = 0.94$ ). The apparent surface concentration of TEMPO units calculated from  $q_a$  corresponds to  $\Gamma_{\text{TU}} = 1.44 \cdot 10^{-10} \text{ mol cm}^{-2}$ , which is in the same order of magnitude but well below sterically limited  $\Gamma$  values reported for monolayers of other redox-active molecules (e.g. ferrocene) covalently attached to smooth surfaces.<sup>[27]</sup> The peak widths at half of the maximum heights ( $W_{1/2}$ ) are significantly smaller than the ideal value of  $90 \text{ mV}$ .<sup>[25]</sup>

By subtracting the film voltammogram from the one measured in TPMA solution, a correction for adsorption contributions was attempted (Figure 4C, orange line). The resulting profile exhibits a  $\Delta E_p$  of  $34 \text{ mV}$ . This value is significantly higher than the  $\Delta E_p$  of the uncorrected CV ( $20 \text{ mV}$ ), but still well below the  $57 \text{ mV}$  expected for a purely diffusive process. Considering that for other redox-active polymers, e.g.

**Table 3.** Analysis of the TPMA film CV recorded at  $v = 1 \text{ Vs}^{-1}$  (see Figure 4C).

Peak	$E_p$ [V]	$q$ [ $10^{-7} \text{ C}$ ]	$j_p$ [ $\text{mA cm}^{-2}$ ]	$W_{1/2}$ [mV]
anodic	0.44	2.79	0.35	46
cathodic	0.43	2.86	0.33	49



linear chains carrying ferrocene, anthraquinone, or tris (dialkylamino)cyclopropenium units,  $\Delta E_p$  values of 60 mV and higher have been reported,<sup>[28]</sup> the behavior of TPMA is quite unusual. While investigations of the unusual peak-to-peak separation are ongoing, it can already be concluded from the results presented in this section that i) the high molecular weight of TPMA reduces the diffusion-controlled current compared to TEMPO and ACT, ii) TPMA forms a redox-active film by irreversible adsorption on the glassy carbon surface, iii) the voltammetric profiles of TPMA are shaped both by diffusive and adsorptive processes, and iv) the influence of adsorbed TPMA becomes negligible at low  $\nu$  and high  $c_{TU}$ .

### 1.3. Electrocatalytic Studies

We continued our investigations by characterizing the electrocatalytic behavior of TPMA. A comparison between the voltammetric profiles of TPMA, ACT, and TEMPO recorded at  $100 \text{ mV s}^{-1}$  in the absence and presence of 4-methoxybenzyl alcohol (4-MBA) is depicted in Figure 5. To facilitate alcohol oxidation, *N*-methylimidazole (NMI) was added as a proton scavenger. A separate CV recorded in absence of any mediator confirmed that direct alcohol oxidation does not proceed in the studied potential regime (see Figure S24). Interestingly, the catalytic peak current density ( $j_{cat}$ ) for TPMA is slightly higher than for TEMPO, but well below the value of ACT. Moreover, the ratio  $j_{cat}/j_p$  that reflects the rate of the homogeneous reaction, is significantly higher for TPMA (9.6) as compared to TEMPO (2.5). In our previous work,<sup>[12]</sup> we attributed this observation to the electron-withdrawing acyloxy linker in position 4 of the piperidiny ring, the resulting increase of the redox potential and thereby to a higher driving force for alcohol oxidation. This conjecture is supported by the similar magnitude of the  $j_{cat}/j_p$  values of TPMA and ACT (9.6 and 7.8), which would also be in line with a previous report by Rafiee, Stahl et al. that highlights the strong influence of the redox potential on the electrocatalytic activity of *N*-oxyl radicals.<sup>[22]</sup>

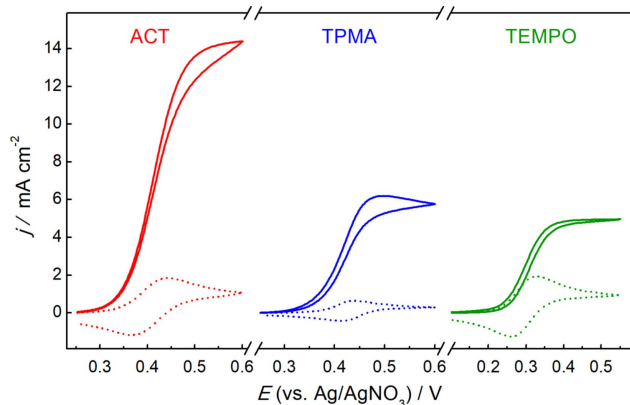


**Figure 5.** Comparison between background-corrected CVs of ACT (left), TPMA (middle), and TEMPO (right) under non-catalytic and catalytic conditions ( $c_{TU} = 5 \text{ mM}$ ,  $\nu = 100 \text{ mV s}^{-1}$ ). Electrolyte:  $0.1 \text{ M NBu}_4\text{ClO}_4$  in acetonitrile/water (8:1). Substrate:  $0.1 \text{ M}$  4-methoxybenzyl alcohol (4-MBA). Base:  $0.45 \text{ M NMI}$ .

For a quantitative treatment of the kinetics of the catalytic process,  $\nu$  was systematically increased to achieve “no substrate consumption – pure kinetic conditions”<sup>[29,30]</sup> with S-shaped voltammetric profiles (for details see the SI). For homogeneous electrocatalysts, the corresponding plateau current densities ( $j_{max}$ ) are given by Eq. 2,

$$j_{max} = zFc_{TU}\sqrt{nDk_{cat}c_{sub}} \quad (2)$$

where  $k_{cat}$  is the homogeneous rate constant,  $n$  the number of catalyst units required per turnover, and  $c_{sub}$  the substrate concentration (the other parameters are defined above). A comparison between the catalytic responses of ACT and TPMA is shown in Figure 6A and B. Linear correlations between  $j_{max}$  and  $c_{TU}$  as well as between  $j_{max}$  and  $\sqrt{c_{sub}}$  (Figure 6C and D) suggests that i) the TPMA-catalyzed process is at least to a large extent a homogeneous one,<sup>[31]</sup> ii) ACT- and TPMA-catalyzed alcohol oxidation is first order both in catalyst and substrate, and iii), ACT renders higher  $j_{max}$  values over the entire  $\nu$  and  $c$  regimes.

The homogeneous rate constants  $k_{cat}$  calculated from the  $j_{max}$  values (for details see the SI) amount to  $397 \text{ L mol}^{-1} \text{ s}^{-1}$  for TPMA and  $330 \text{ L mol}^{-1} \text{ s}^{-1}$  for ACT. In comparison, the value for TEMPO ( $24 \text{ L mol}^{-1} \text{ s}^{-1}$ ) turns out to be much lower, confirming that the homogeneous rate of alcohol oxidation is determined by the redox potential of the TEMPO unit rather than by its attachment to the polymer backbone. To generalize the comparison between the polymediator and the low-molecular weight benchmark systems, the catalytic study was extended to 5-(hydroxymethyl)furfural (HMF), glycerol, methanol and prop-

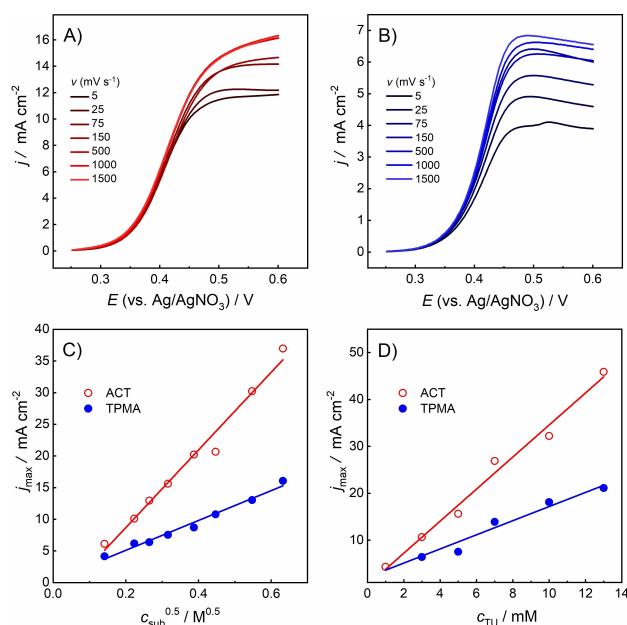


**Figure 6.** Top: Background-corrected catalytic profiles of  $5 \text{ mM}$  ACT (A) and  $5 \text{ mM}$  TPMA (B) in presence of  $0.1 \text{ M}$  4-MBA and  $0.45 \text{ M}$  *N*-methylimidazole (NMI) at varying scan rates. Bottom: Comparison between the achievable  $j_{max}$  values of ACT and TPMA at varying substrate concentrations (C) and varying concentrations of TEMPO units (D). Electrolyte:  $0.1 \text{ M NBu}_4\text{ClO}_4$  in acetonitrile/water (8:1).

an-2-ol (see Figure 7 and the SI). In all of these cases, ACT and TPMA exhibit similar rate constants, whereas TEMPO shows comparatively low  $k_{\text{cat}}$  values (Figure 7B).

Considering the similarity between ACT and TPMA, the impression that the homogeneous kinetics are not strongly affected by the active centers being attached to the polymer backbone thus seems to be strengthened. In other words, the TEMPO units on the polymer appear to be well accessible for the substrate and thus available for catalysis. Furthermore, it is worth mentioning that in the cases of 4-MBA, HMF, methanol and glycerol, despite the much lower diffusion coefficient, the  $j_{\text{max}}$  values of TPMA are significantly higher than the ones of TEMPO. Thus, in these cases, the higher driving force trumps the curbed mediator transport, leading to more efficient overall kinetics.

## 2. Conclusions

In the present study, progress was made in understanding the redox behavior and catalytic activity of TEMPO-modified polymethacrylates in view of their application as mediators in electrosynthesis. It was found that the polymer tends to irreversibly adsorb on glassy carbon, thus forming a redox-

active layer on the electrode surface. These layers have a pronounced influence on the voltammetric profiles at high scan rates and low mediator concentrations. Electrocatalytic studies at varying concentrations of alcohol substrate and TEMPO units suggest that TPMA-catalyzed alcohol oxidation is a predominantly homogeneous process.

Although TPMA shows significantly slower diffusive behavior compared to TEMPO and ACT, the catalytic current densities achievable with the polymer are intermediate between those of the two low molecular weight mediators for the majority of substrates. Since the homogeneous rate constants of TPMA and ACT resemble each other, being well above the ones of TEMPO for the tested substrates, it can be concluded that the redox potential of the *N*-oxyl unit has a more pronounced effect on the rate of the homogeneous reaction than the active centers being attached to the polymer backbone. This means that curbed mass transfer can be compensated by tuning the redox potential of the catalyst unit, which should be considered as an important design principle for the development of new polymediator generations. Tuning the molecular weight distribution may represent a further possibility for optimization of the overall reaction rate, which is currently under investigation in our laboratory.

## Acknowledgements

This work has been funded by the German Research Foundation (DFG, project no. FR 3848/2-1). The author is grateful for funding by the DFG Heisenberg Program (FR 3848/4-1). Furthermore, we thank Alina Heckel and Dr. Lutz Nuhn from the Max Planck Institute for Polymer Research (Mainz, Germany) for their helpful support in polymer characterization by size exclusive chromatography. Open Access funding enabled and organized by Projekt DEAL.

## Conflict of Interest

The authors declare no conflict of interest.

**Keywords:** electrosynthesis · electrocatalysis · mediator · TEMPO · polymer

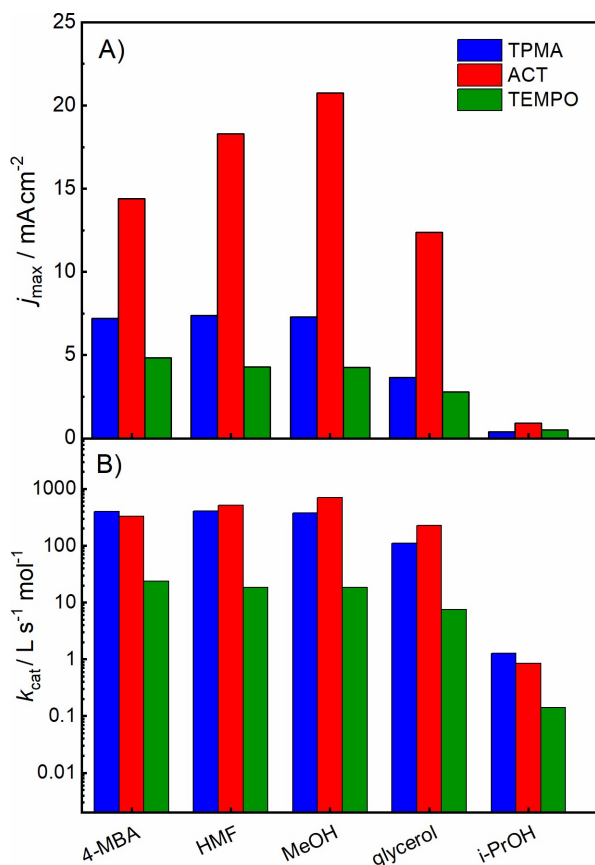


**Figure 7.** Comparison between the catalytic activities of TPMA, ACT and TEMPO for various substrates. Top: Plateau current densities ( $j_{\text{max}}$ ) achieved under “no substrate consumption – pure kinetic conditions” ( $c_{\text{sub}} = 5$  mM,  $c_{\text{sub}} = 0.1$  M). Bottom: Rate constants  $k_{\text{cat}}$  calculated from the  $j_{\text{max}}$  values.

- [1] E. Steckhan, *Angew. Chem. Int. Ed. Engl.* **1986**, *25*, 683.
- [2] R. Francke, R. D. Little, *Chem. Soc. Rev.* **2014**, *43*, 2492.
- [3] a) L. Ackermann, *Acc. Chem. Res.* **2020**, *53*, 84; b) J. C. Siu, N. Fu, S. Lin, *Acc. Chem. Res.* **2020**, *53*, 547; c) C. Ma, P. Fang, T.-S. Mei, *ACS Catal.* **2018**, *8*, 7179; d) J. Strehl, G. Hilt, *Org. Lett.* **2019**, *21*, 5259; e) S. Tang, D. Wang, Y. Liu, L. Zeng, A. Lei, *Nat. Commun.* **2018**, *9*, 798; f) B. R. Walker, S. Manabe, A. T. Brusoe, C. S. Sevov, *J. Am. Chem. Soc.* **2021**, *143*, 6257.
- [4] a) P. Qian, Z. Zha, Z. Wang, *ChemElectroChem* **2020**, *7*, 2527–2544; b) Y. N. Ogibin, M. N. Elinson, G. I. Nikishin, *Russ. Chem. Rev.* **2009**, *78*, 89.
- [5] a) C.-Y. Cai, X.-M. Shu, H.-C. Xu, *Nat. Commun.* **2019**, *10*, 4953; b) N.-n. Lu, N.-t. Zhang, C.-C. Zeng, L.-M. Hu, S. J. Yoo, R. D. Little, *J. Org. Chem.* **2015**, *80*, 781; c) Y. S. Park, R. D. Little, *J. Org. Chem.* **2008**, *73*, 6807.
- [6] a) M. Elsherbini, T. Wirth, *Chem. Eur. J.* **2018**, *24*, 13399; b) R. Francke, *Curr. Opin. Electrochem.* **2019**, *15*, 83; c) R. Francke, *Curr. Opin. Electrochem.* **2021**, *28*, 100719.

- [7] a) A. Das, S. S. Stahl, *Angew. Chem. Int. Ed.* **2017**, *56*, 8892; b) M. Rafiee, Z. M. Konz, M. D. Graaf, H. F. Koolman, S. S. Stahl, *ACS Catal.* **2018**, *8*, 6738; c) J. E. Nutting, M. Rafiee, S. S. Stahl, *Chem. Rev.* **2018**, *118*, 4834; d) H.-B. Zhao, P. Xu, J. Song, H.-C. Xu, *Angew. Chem. Int. Ed.* **2018**, *57*, 15153; e) D. P. Hickey, D. A. Schiedler, I. Matanovic, P. V. Doan, P. Atanassov, S. D. Minteer, M. S. Sigman, *J. Am. Chem. Soc.* **2015**, *137*, 16179.
- [8] R. Francke, *Chimia* **2020**, *74*, 49.
- [9] a) T. Sawamura, S. Kuribayashi, S. Inagi, T. Fuchigami, *Org. Lett.* **2010**, *12*, 644; b) T. Broese, R. Francke, *Org. Lett.* **2016**, *18*, 5896; c) O. Koleda, T. Broese, J. Noetzel, M. Roemelt, E. Suna, R. Francke, *J. Org. Chem.* **2017**, *82*, 11669; d) A. F. Roesel, T. Broese, M. Májek, R. Francke, *ChemElectroChem* **2019**, *6*, 4229.
- [10] T. Sawamura, S. Kuribayashi, S. Inagi, T. Fuchigami, *Adv. Synth. Catal.* **2010**, *352*, 2757.
- [11] a) H. Tanaka, J. Chou, M. Mine, M. Kuroboshi, *Bull. Chem. Soc. Jpn.* **2004**, *77*, 1745; b) M. Kuroboshi, K. Goto, H. Tanaka, *Synthesis* **2009**, 903.
- [12] B. Schille, N. O. Giltzau, R. Francke, *Angew. Chem. Int. Ed.* **2018**, *57*, 422.
- [13] J. Wang, *Analytical Electrochemistry (3<sup>rd</sup> Edition)*, Wiley-VCH, **2006**.
- [14] a) For the synthesis of HP-2, a modified procedure from Ref. [14b] was used; b) T. Janoschka, N. Martin, U. Martin, C. Friebe, S. Morgenstern, H. Hiller, M. D. Hager, U. S. Schubert, *Nature* **2015**, *527*, 78.
- [15] During conversion of **2** to the TEMPO-modified polymethacrylate, the intermediate precipitates from the aqueous solution prior to complete oxidation. Therefore, the solid is filtered off and dissolved in THF, where the conversion is brought to completion in presence of MCPBA.
- [16] T. Janoschka, A. Teichler, A. Krieg, M. D. Hager, U. S. Schubert, *J. Polym. Sci. Part A* **2012**, *50*, 1394.
- [17] Direct comparison between the  $M_w$  values of HP-2 from Ref. [12] and TPMA is difficult, since different SEC systems and standards were used for SEC measurements.
- [18] a) C. P. Jesson, C. M. Pearce, H. Simon, A. Werner, V. J. Cunningham, J. R. Lovett, M. J. Smallridge, N. J. Warren, S. P. Armes, *Macromolecules* **2017**, *50*, 182; b) D. B. Thomas, A. J. Conventine, R. D. Hester, A. B. Lowe, C. L. McCormick, *Macromolecules* **2004**, *37*, 1735.
- [19] V. V. Pavlishchuk, A. W. Addison, *Inorg. Chim. Acta* **2000**, *298*, 97.
- [20] It should be noted that for the calculation of  $c_{TU}$ , the end groups on the polymer chains could not be taken into account, potentially leading to an overestimation of the actual concentration. However, in view of the relatively high molecular weight of TPMA, we assume that this effect is rather small.
- [21] R. F. Winter, *Organometallics* **2014**, *33*, 4517.
- [22] M. Rafiee, K. C. Miles, S. S. Stahl, *J. Am. Chem. Soc.* **2015**, *137*, 14751.
- [23] R. S. Nicholson, I. Shain, *Anal. Chem.* **1964**, *36*, 706.
- [24] A slight underestimation of the transferred charge equivalents may result from an overestimation of  $c_{TU}$  (see Ref. [20]).
- [25] A. J. Bard, L. R. Faulkner, *Electrochemical Methods. Fundamentals and Applications*, Wiley, New York, **2001**.
- [26] a) G. Nagarjuna, J. Hui, K. J. Cheng, T. Lichtenstein, M. Shen, J. S. Moore, J. Rodríguez-López, *J. Am. Chem. Soc.* **2014**, *136*, 16309; b) E. C. Montoto, Y. Cao, K. Hernández-Burgos, C. S. Sevov, M. N. Braten, Brett A. Helms, J. S. Moore, J. Rodríguez-López, *Macromolecules* **2018**, *51*, 3539; c) M. Yuan, S. D. Minteer, *Curr. Opin. Electrochem.* **2019**, *14*, 1.
- [27] a) B. M. Johnson, R. Francke, R. D. Little, L. A. Berben, *Chem. Sci.* **2017**, *8*, 6493; b) M. A. Pellow, T. D. P. Stack, C. E. D. Chidsey, *Langmuir* **2013**, *29*, 5383; c) M. V. Sheridan, K. Lam, W. E. Geiger, *Angew. Chem. Int. Ed.* **2013**, *52*, 12897.
- [28] a) J. B. Flanagan, S. Margel, A. J. Bard, F. C. Anson, *J. Am. Chem. Soc.* **1978**, *100*, 4248; b) B. L. Funt, P. M. Hoang, *J. Electrochem. Soc.* **1984**, *131*, 2295; c) K. H. Hendriks, S. G. Robinson, M. N. Braten, C. S. Sevov, B. A. Helms, M. S. Sigman, S. D. Minteer, M. S. Sanford, *ACS Cent. Sci.* **2018**, *4*, 189.
- [29] J.-M. Savéant, *Chem. Rev.* **2008**, *108*, 2348.
- [30] J.-M. Savéant, K. B. Su, *J. Electroanal. Chem.* **1984**, *171*, 341.
- [31] a) For substrate conversion at active centers attached to the electrode surface, a linear dependency of  $j_{max}$  on  $c_{sub}$  is expected (see Ref. [25] and Ref. [31b]); b) C. Costentin, J.-M. Savéant, *J. Phys. Chem. C* **2015**, *119*, 12174.

Manuscript received: June 4, 2021

Revised manuscript received: June 23, 2021

Accepted manuscript online: June 25, 2021